

MESENCHYMAL STEM CELLS THERAPY FOR THIOACETAMIDE INDUCED LIVER CIRRHOSIS**ZAKARIA EL-KHAYAT¹, EHAB MOSTAFA², JIHAN HUSSEIN^{1*}, MAHA EL-WASEEF¹, LAILA. RASHED³, ABDEL RAZIK FARRAG⁴, DALIA MEDHAT¹**¹Medical Biochemistry Department, National Research Center, Doki, Giza, Egypt, ²Biochemistry Department, Faculty of Science, Tanta University, Tanta, Egypt, ³Biochemistry Department, Faculty of Medicine, Cairo University, ⁴Pathology Department National Research Centre, Doki, Giza, Egypt. Email: jihan_husein@yahoo.com.*Received: 16 Feb 2013, Revised and Accepted: 01 Apr 2013***ABSTRACT**

Objective: Hepatic cirrhosis is the end stage of chronic liver disease, the majority of patients with cirrhosis die from life threatening complications. Recently, Mesenchymal stem cells show ability to differentiate into hepatocytes, stimulate the regeneration of endogenous parenchymal cells and enhance fibrous matrix degradation. Thus, this study aimed to evaluate the possible therapeutic effect of mesenchymal stem cells in thioacetamide (TAA) induced liver cirrhosis in rats.

Methods: Animal model of liver cirrhosis was induced by intraperitoneal injection of thioacetamide in a dose of 150mg/kg body weight, twice a week for 14 weeks. Ten male albino rats weighting 100-120 g were used for isolation of bone marrow derived mesenchymal stem cells (BM-MSCs) and thirty-five healthy female albino rats weighting 150-200 g were divided into three groups; control, cirrhotic and treated groups. After the experimental period, blood samples were withdrawn from the retro orbital vein plexus for estimation of liver functions, liver tissue was collected for determination of hydroxyproline content, collagen gene expression and histological examination.

Results: Results showed that administration of BM-MSCs improved liver functions and reduced hydroxyproline content. Histological examination of liver tissue showed a significant antifibrotic effect in treated group as evidenced by the disappearance of septal collagen deposition.

Conclusion: therapeutic potential of MSCs with injured liver tissue represents a novel strategy to augment the differentiation ability of cells towards hepatic lineage. Furthermore, MSCs demonstrated better survival, proliferation, differentiation and functional abilities for hepatocytes.

Keywords: Stem cells, Cirrhosis, Thioacetamide, Bone marrow, Hydroxyproline

INTRODUCTION

Liver has a prominent role in the regulation of physiological processes. It is involved in varieties of vital functions such as metabolism, secretion and storage. Furthermore, detoxification of a variety of drugs and xenobiotics occurs in liver. Hence liver diseases are among the most serious health problems. They may be classified as acute or chronic hepatitis (inflammatory liver diseases), hepatitis (non inflammatory diseases) and cirrhosis (degenerative disorder resulting in fibrosis of the liver). Liver diseases are mainly caused by toxic chemicals (certain antibiotics, chemotherapeutics, peroxidised oil, aflatoxin, carbon-tetrachloride, paracetamol, chlorinated hydrocarbons, etc.), excess consumption of alcohol, infections and autoimmune disorder [1].

Liver failure is a potentially life-threatening condition for which organ transplantation is the only definitive therapy [2]. However, the current shortage of available livers for transplantation results in the death of many patients while awaiting transplantation [3]. A logical alternative would be to isolate and transplant human hepatocytes. Unfortunately, isolation of human hepatocytes is difficult and inefficient [4]. Therefore, stem cells can be readily isolated using non invasive procedures to give rise to hepatocytes [5].

Stem cells have potential in several regions of medical research. One probable application is to make new cells and tissues for medical therapies. Such as, donated organs and tissues are frequently used to exchange those that are diseased or destroyed. Inappropriately, the number of individuals suffering from diseases that might benefit from stem cell therapy is much greater than the number of organs and tissues available for transplantation. Stem cells suggest the probability of renewable sources of auxiliary cells and new tissues to treat many kinds of diseases, conditions, and disabilities [6].

Bone marrow considered as a transplantable source of hepatic progenitors. Initial reports of the hepatic potential of haematopoietic stem cells were later shown to have resulted from fusion between transplanted donor cells and resident recipient hepatocytes [7]. Mesenchymal stem cells (MSCs) constitute a bone marrow-derived stem cell population that has been shown to have therapeutic potential in a wide range of diseases [8].

Hepatic fibrosis or cirrhosis results from the imbalance of extracellular matrix (ECM) production and degradation. Any approach that resets the balance could lead to the resolution of fibrogenic liver disorders. The fact that MSC have antifibrosis effects in injured liver has been clearly demonstrated in animal models of liver fibrosis [9].

Thus, the aim of this study was to evaluate the possible therapeutic effect of mesenchymal stem cells in thioacetamide induced liver cirrhosis in rats.

MATERIALS AND METHODS**Materials****Chemicals**

Thioacetamide (TAA), Chloramine T, p-dimethylaminobenzaldehyde, acid soluble collagen and hydroxyproline were purchased from Sigma Chemical Company (St. Louis, U.S.A) sodium acetate, citric acid, perchloric acid, n-propanol, sodium hydroxide, acetic acid were purchased from Fisher Scientific (St. Louis, U.S.A). Dulbecco's modified Eagle's medium (DMEM), Streptomycin and Penicillin, Fetal bovine serum (FBS) and 0.25% trypsin in 1mM (Ethylenediaminetetraacetic acid) EDTA were purchased from (GIBCO/BRL). Agarose (Ultra-pure agarose, electrophoresis grade), bromophenol blue, Ethidium bromide (EB), Tris-Acetate EDTA buffer (TAE), glycerol, xylene cyanol and gel control DNA marker were purchased from Ferments, Italy. Moloney murine leukemia virus (MMLV) reverse transcriptase, Human Placental Ribonuclease Inhibitor (HPRI), Deoxynucleotide triphosphate, First strand buffer, Random hexamers and DEPC- treated water were purchased from Ferments, Italy. Thermus aquaticus (Taq) DNA polymerase, Taq buffer, dNTPs and CD29 biotinylated primers were purchased from Ferments, Italy.

Experimental animals

Ten male albino rats weighting 100-120 g and thirty-five female albino rats weighting 150-200 g were obtained from the animal house of the National Research Center. Rats were bred and

maintained in an air-conditioned animal house with specific pathogen free conditions, and were subjected to a 12:12 h daylight/darkness and allowed unlimited access to chow and water. All the ethical protocols for animal treatment were followed and supervised by the animal facilities, National Research Center, Cairo. All animal experiments received approval from the animal care committee, National Research Center.

Methods

Induction of cirrhosis

Induction of cirrhosis in this study was done and modified from the method described by [10]. The animal model of cirrhosis was induced by intraperitoneal injection of Thioacetamide (TAA) in a dose of 150 mg/kg body weight twice a week for 14 weeks and then 5 animals were sacrificed and pathological examination of liver was done to ensure cirrhosis induction.

Preparation of BM-derived MSC

Bone marrow was harvested by flushing the tibiae and femurs of 6 weeks-old male rats with Dulbecco's modified Eagle's medium (DMEM, GIBCO/BRL) supplemented with 10% fetal bovine serum (GIBCO/BRL). Nucleated cells were isolated with a density gradient [Ficoll/Paque (Pharmacia)] and resuspended in complete culture medium supplemented with 1% penicillin-streptomycin (GIBCO/BRL). Cells were incubated at 37 °C in 5% humidified CO₂ for 12–14 days as primary culture or upon formation of large colonies. When large colonies developed (80–90% confluence), cultures were washed twice with phosphate buffer saline (PBS) and the cells were trypsinized with 0.25% trypsin in 1mM EDTA (GIBCO/BRL) for 5 min at 37 °C. After centrifugation, cells were resuspended with serum-supplemented medium and incubated in 50 cm² culture flask (Falcon). The resulting cultures were referred to as first-passage cultures [11]. MSCs in culture were characterized by their adhesiveness and fusiform shape [12] and by expression of CD29 as a surface marker of MSCs according to [13].

RT-PCR detection of CD29 gene expression

Total RNA was extracted from cells using RNeasy Purification Reagent (Qiagen, Valencia, CA), and then a sample (1 µg) was reverse transcribed with reverse transcriptase (RT) for 30 min at 42 °C in the presence of oligo-dT primer. Polymerase chain reaction (PCR) was performed using specific primers (UniGene Rn.25733) forward: 5'-AATGTTTCAGTGCAGAGC-3' and reverse:

5'-TTGGGATGATGTCGGGAC-3'. PCR was performed for 35 cycles, with each cycle consisting of denaturation at 95 °C for 30 s, annealing at 55 °C to 63 °C for 30 s and elongation at 72 °C for 1 min, with an additional 10- min incubation at 72 °C after completion of the last cycle. To exclude the possibility of contaminating genomic DNA, PCRs were also run without RT. The PCR product was separated by electrophoresis through a 1% agarose gel, stained, and photographed under ultraviolet light [14].

Labeling of stem cells with PKH26 dye

MSCs were harvested during the 4th passage and were labeled with PKH 26 fluorescent linker dye according to Sigma protocol (Saint Louis, Missouri USA). Briefly, Cells were centrifuged and washed twice in serum free medium. Cells were pelleted and suspended in dye solution; the cells were injected intravenously into rat tail vein [15].

Experimental design

30 female albino rats were divided into 3 groups as follows: Group I (Control group): 10 healthy rats received phosphate buffer saline (150 mg/kg body weight) intravenously infusion at the tail vein. Group II (Cirrhotic group): 10 cirrhotic rats received phosphate buffer saline intravenous infusion at the tail vein. Group III (Treated group): cirrhotic rats injected with MSCs in a single dose of 10⁶ cells per rat by intravenous infusion at the tail vein [16].

After 4 weeks of MSCs administration, venous blood was collected from the retro-orbital vein from rats of all groups. All rats were sacrificed with the cervical dislocation, and the liver tissue was harvested for histopathological and histochemical examination.

Homing detection of MSCs in liver tissue

Liver tissue was examined with a fluorescence microscope to detect and trace the cells stained with PKH26.

Determination of liver functions in serum

Serum ALT and AST were determined according to [17], also serum albumin and total protein levels were estimated according to [18] and [19] respectively. In addition, A/G ratio was calculated.

Hydroxyproline (Hyp) content assay

A colorimetric assay was performed according to [20]. Briefly, liver sections (0.5 g) were hydrolyzed (20 h in 6 mol/L HCl at 100 °C), redissolved in water and centrifuged to remove any impurities. Samples were incubated for 10 min in 0.05 mol/L chloramine-T (Fisher, Fair Lawn, NJ, USA) at room temperature, followed by 15 min incubation in Ehrlich's perchloric acid solution at 65 °C. Sample absorbance was assessed at 561 nm and resulting values compared to a Hyp standard curve. Each sample was assayed in duplicate. The Hyp content was expressed as micrograms per gram of wet liver.

Semi-quantitative RT-PCR detection of collagen gene II expression

Total RNA was extracted from liver tissue homogenate using RNeasy purification reagent (Qiagen, Valencia, CA). cDNA was generated from 5 µg of total RNA extracted with 1 µl (20 pmol) antisense primer and 0.8 µl superscript AMV reverse transcriptase for 60 min at 37 °C. For PCR, 4 µl cDNA was incubated with 30.5 µl water, 4 µl 25mM MgCl₂, 1 µl dNTPs (10 mM), 5 µl 10× PCR buffer, 0.5 µl (2.5 U) Taq polymerase and 2.5 µl of each primer containing 10 pmol. Primer sequences were as follows: forward 5'-GCCCATGATACTAAGTGAGAAATAC-3', reverse 5'-GTAAAACGTGAAACAATCCTAAGA-3'. The reaction mixture was subjected to 40 cycles of PCR amplification as follows: denaturation at 95 °C for 1 min, annealing at 67 °C for 1 min and extension at 72 °C for 2 min. To exclude the possibility of contaminating genomic DNA, PCRs were also run without RT. The PCR product yielded a 333 bp fragment on 1.5% agarose gel electrophoreses [21].

Semi-quantitation was performed using the gel documentation system (BioDO, Analyser) supplied by Biometra according to the following amplification procedure: relative expression of each studied gene (R) was calculated following the formula: R = Densitometrical Units of each studied gene / Densitometrical Units of β-actin.

PCR detection of β-actin

The presence of RNA in all tissues was assessed by analysis of the "house-keeping" gene β-actin. cDNA was generated from 1 µg of total RNA extracted with AMV reverse transcriptase for 60 min at 37 °C. For PCR, 4 µl cDNA was incubated with 30.5 µl water, 4 µl 25 mM MgCl₂, 1 µl dNTPs (10 mM), 5 µl 10× PCR buffer, 0.5 µl (2.5 U) Taq polymerase and 2.5 µl of each primer containing 10 pmol. β-actin primers (forward 5'-TGTTGTCCCTGTATGCCTCT-3', reverse

5'-TAATGTCACGCACGATTTC-3') were designed from GenBank (accession no.J00691). The reaction mixture was subjected to 40 cycles of PCR amplification as follows: denaturation at 95 °C for 1 min, annealing at 57 °C for 1 min and extension at 72 °C for 2 min. The PCR product yielded 206 bp fragments.

Histological and histochemical examinations

Liver specimens were taken immediately after the rats were sacrificed and stained according to [22]. Glycogen storage ability of hepatocytes was analyzed, Quantitative measurement of the severity of liver fibrosis, and glycogen were achieved by using computerized image analyzer (Leica Qwin 500 image).

Statistical analysis

The results were expressed as the mean ± S.E. Comparisons were made among the groups using ANOVA followed by *t* test (Origin Lab publishes graphing and data analysis software version 4.0) at the selected level of significance.

RESULTS

Identification and homing of BM-MSCs

Bone marrow derived mesenchymal stem cells were identified by their adhesiveness and fusiform shape (Figure 1). Also, CD29 gene expression by RT-PCR was detected as a marker of MSCs (Figure 2).

Homing of MSCs into liver tissue was confirmed by labeled MSCs with the PKH26 dye, these cells showed strong red auto fluorescence after transplantation into rats, confirming that these cells were actually seeded into the liver tissue (Figure 3).

MSCs administration improves liver functions

This study showed that serum ALT and AST activities were increased significantly ($P < 0.05$) in cirrhotic group compared to the

control group while these values were significantly decreased in treated group and return to the normal levels (Table 1).

The mean values of serum albumin and total protein were significantly decreased in cirrhotic group compared to control while these values were significantly increased by MSCs administration compared to the cirrhotic one (Table 1).

Collagen gene expression and hydroxyproline content

In the current study, gene expression analysis by RT-PCR showed elevated level of collagen expression in the cirrhotic group compared to the control group, while this value was significantly decreased in treated group compared to the cirrhotic one. The expression of this gene associated with hydroxyproline content in liver tissue (Table 2, Figure 4).



Fig. 1: Photomicrograph shows the morphology of mesenchymal stem cells (MSCs) from culture.

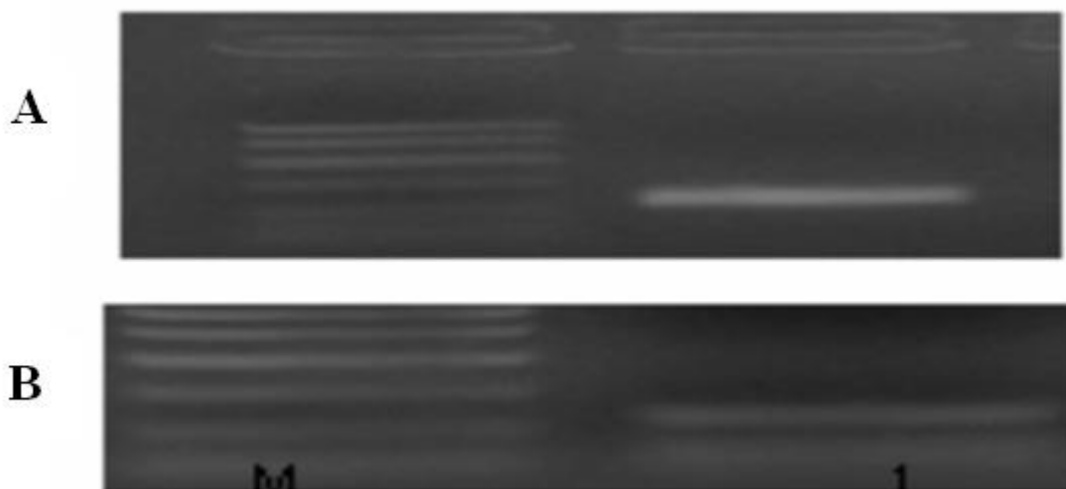


Fig. 2: UV transilluminated agarose gel electrophoresis show PCR products of CD29 of isolated MSCs and β actin. (A) :PCR product of CD29. (B): PCR product of β actin gene (218 bp). Lane M: DNA marker with (100, 200, 300, 700, 1000bp) Lane 1 (A):PCR product of CD29. Lane 1 (B): PCR product of β actin gene.

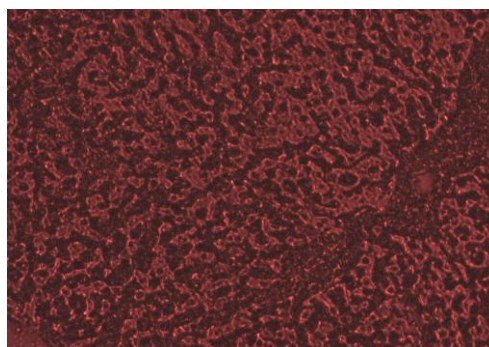


Fig. 3: Photomicrograph shows PKH26 fluorescent staining of cells in the liver tissue.

Table 1: Liver functions in the different studied groups

Groups		Serum ALT (U/I)	Serum AST (U/I)	Albumin (g/dl)	Total Protein (g/dl)	Globulin (g/dl)	Albumin/ globulin ratio
Control	Mean ± SE	36 ± 0.33	89 ± 0.68	3.9 ± 0.03	7.7 ± 0.1	3.8 ± 0.1	1.0 ± 0.03
Cirrhotic	Mean	46 ± 0.81	104 ± 1.15	3.3 ± 0.04	7.1 ± 0.12	3.8 ± 0.1	0.86 ± 0.03
	± SE	0.000*	0.000*	0.000*	-7.7%	N.S.	0.004*
	<i>P^a</i> value	27%	16.8%	0.000*	-15.3%	0%	16.2 %
	% of change ^a						
Treated	Mean ± SE	33 ± 0.74	85 ± 1.11	3.8 ± 0.03	8 ± 0.12	4.2 ± 0.14	0.92 ± 0.03
	<i>P^a</i> value	0.014*	0.008*	NS	NS	N.S.	N.S.
	<i>P^b</i> value	0.000*	0.000*	0.000*	0.000*	N.S.	N.S.
	% of change ^a	-13.8%	-4.4%	-2.5%	-3.8%	-9.5 %	-8 %
	% of change ^b	-28.2%	-18.2%	15.1%	12.6%	-9.5 %	6.9 %

Significant *P* value < 0.05, NS not significant

P^a value vs. control, *P^b* value vs. cirrhotic

Percent of change ^a: Percent of change from control

Percent of change ^b: Percent of change from cirrhotic

Table 2: Hydroxyproline content and collagen gene expression in the different studied groups

Groups		Hydroxyproline content in liver tissue (µg/g protein)	Relative expression of collagen gene
Control	Mean ± SE	73 ± 1.6	0.13 ± 0.013
Cirrhotic	Mean ± SE	304 ± 16.5	1.54 ± 0.122
	<i>P^a</i> value	0.000*	0.000*
	% of change ^a	316 %	1084.6 %
Treated	Mean ± SE	122 ± 4.3	0.52 ± 0.05
	<i>P^a</i> value	0.001*	0.001*
	<i>P^b</i> value	0.000*	0.000*
	% of change ^a	67 %	300 %
	% of change ^b	-59.8 %	-66 %

Significant *P* value < 0.05, NS not significant

P^a value vs. control, *P^b* value vs. cirrhotic.

% of change ^a: Percent of change from control.

% of change ^b: Percent of change from cirrhotic.

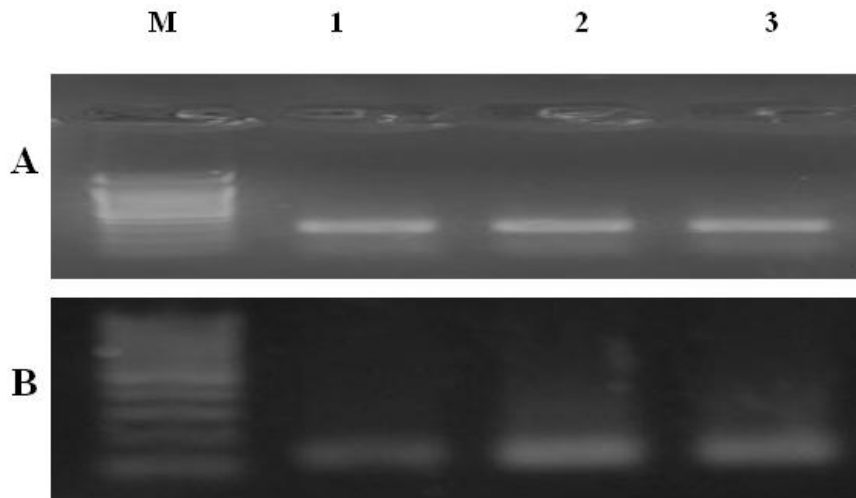


Fig. 4: UV transilluminated agarose gel electrophoresis show PCR products of collagen gene expression in different studied groups. (A) β actin gene (218bp). (P) Lane M: DNA marker with 100bp, Lane 1: PCR products in control group, Lane 2: PCR products in cirrhotic group, and Lane 3: PCR products in treated group.

Histological examination

In this study, histological examination of liver tissue from the control group showed normal structure of hepatic lobules (Figure 5-A). While, the cirrhotic group showed periportal cirrhotic characterized by portal-portal fibrous septa surrounding the hepatic lobules (Figure 5-B) with progress increase in collagen accumulation in the liver (Figure 5-C) as

compare to the control group, while liver examination of the treated group showed an improvement in the hepatic structure as compared to the cirrhotic group (Figure 5-D).

Image analysis of the collagen distribution in liver of the cirrhotic group showed significant increase as compared with the control group. On the other hand, the treated group showed significant decrease as compared with the cirrhotic group (Table 3).

Table 3: Collagen deposition areas in liver of cirrhotic and treated groups

Groups	Area (μm^2)	Area Fraction	Area %
Cirrhotic	518.12 \pm 44.45	0.28 \pm 0.02	27 \pm 2.29
Treated	171.78 \pm 17.69 *	0.01 \pm 0.01	10.106 \pm 1.15

*Significant at $P < 0.05$ as compared with cirrhotic group.

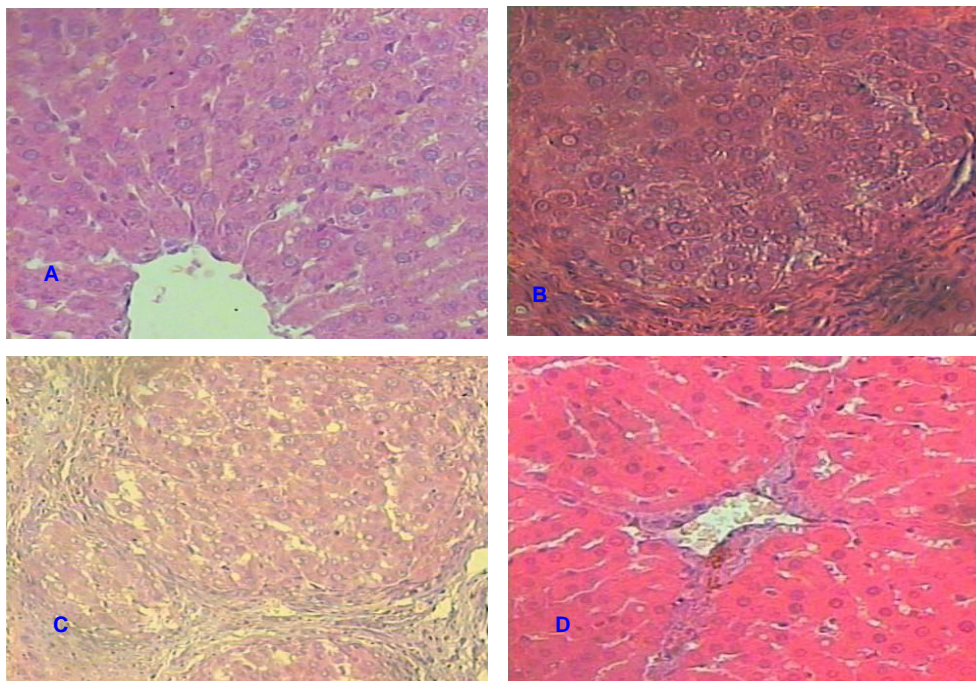


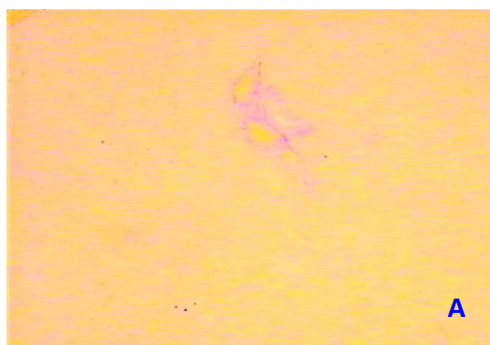
Fig. 5: A photomicrographs of liver A) of control rat shows normal structure of hepatic lobules, B): of cirrhotic group shows coagulation necrosis of hepatocytes that occurred primarily in centrilobular. Infiltration of macrophages and lymphocytes was seen in areas of hepatic injury, C): of cirrhotic group shows fibrosis that evidenced by fibrotic septum formation starting in the portal areas and D): of rat treated group showed an improvement in the hepatic lobule. The areas of hepatocytes necrosis were replaced by normal appearing hepatic architecture; thickened septal cirrhotic became thinner or disappeared (H & E stain $\times 300$).

Liver stained with Van Gieson's stain showed a normal distribution of collagen deposition in the control group (Figure 6-A), although, in case of cirrhotic group, collagen accumulation was significant increased as compared with control one (Figure 6-B). On the other hand, septal collagen deposition disappeared or became thinner in the treated group (Figure 6-C).

The hepatocytes that stained with PAS stain for glycogen revealed normal distribution in the control rats (Figure 7-A). Loss of glycogen

in the hepatocytes of the cirrhotic group was present (Figure 7-B). Liver sections from treated group showed diffuse and homogeneous PAS staining for glycogen (Figure 7-C).

The grey levels of glycogen distribution in liver of control, cirrhotic and treated groups were presented in table (4). The results showed a significant decrease in glycogen in the cirrhotic group as compared to control group. The treated group showed significant increase of the glycogen as compared to the cirrhotic group.



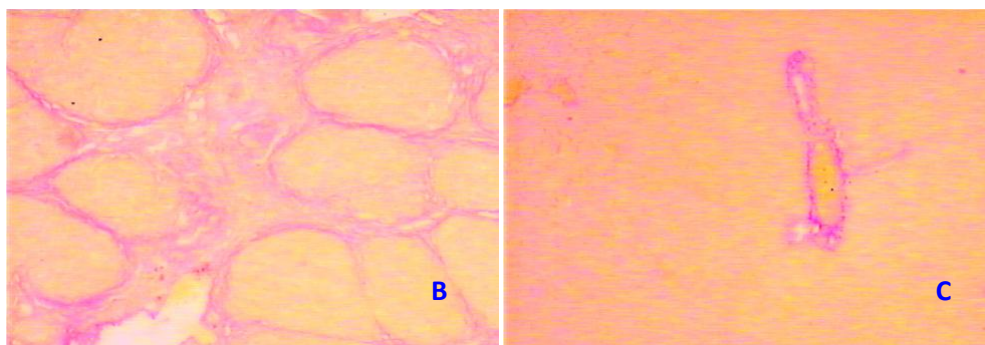


Fig. 6: Photomicrographs of liver A) of the control group shows normal distribution of collagen deposition, B): of the cirrhotic group shows a progress increase in collagen accumulation in the liver, with periportal cirrhotic characterized by portal-portal fibrous septa surrounding the hepatic lobules, and C): of the treated group shows disappearance of septal collagen deposition as compared with that treated with thioacetamide (Van Gieson's staining x 300).

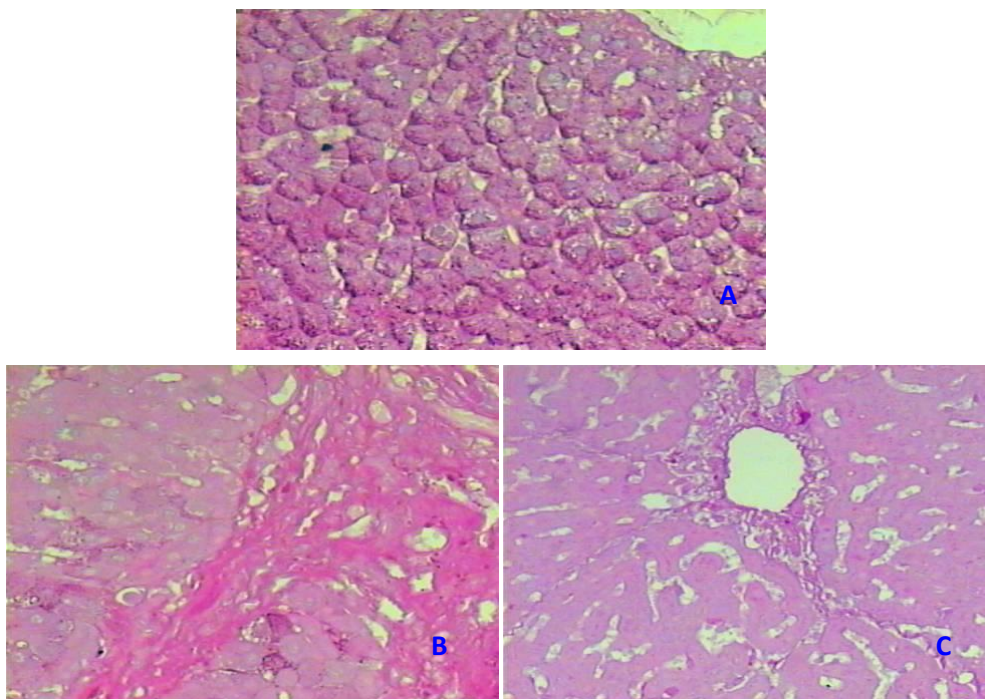


Fig. 7: A photomicrographs of liver of rats shows A): the normal distribution of glycogen in the hepatocytes of the control rat, B): depletion of glycogen of the hepatocytes of the cirrhotic rat, and C): the diffusion and homogeneous of the glycogen hepatocytes of the treated rat (PAS staining x 300).

Table 4: Grey levels of glycogen distribution in liver of different studied groups

Groups	Grey levels of glycogen distribution
Control	112.18 ± 3.04
Cirrhotic	233.34 ± 2.29*
Treated	159.41 ± 1.36**

*Significant at $P < 0.05$ as compared with control group; **Significant at $P < 0.05$ as compared with the cirrhotic group

DISCUSSION

In this study, TAA administration results in deficiencies in liver functions and a progress increase in collagen accumulation in the liver with periportal cirrhotic characterized by portal-portal fibrous septa surrounding the hepatic lobules.

These results were in agreement with [23] who indicated that TAA-induced cirrhosis characterized by cellular necrosis, fibrosis, micronodular reorganization of the parenchyma, duct proliferation, transaminase increase, peroxidation of lipid membranes, and macronodular cirrhosis.

The proposed initiation of cellular events chain leading to xenobiotic- induced liver necrosis is due to reactive metabolites

derived from biotransformation of chemical agents. The active metabolites responsible for hepatotoxicity of thioacetamide are those derived from thioacetamide S-oxide, the product of oxidation of thioacetamide by FAD-monoxygenase system. The free radicals generated by this oxidative pathway cause lipid peroxidation, glutathione depletion and a reduction in SH-thiol groups. The selective destruction of liver cells in the perivenous necrosis is followed immediately by a proliferative process that reaches its maximum at 48 h in 2-month-old rats after thioacetamide administration, and at 72 h in 6- to 30-month-old animals [24].

In the current study, BM-MSCs were isolated from adult male rats, characterized in culture by their adhesiveness and fusiform shape. CD29 gene expression as a marker of MSCs was also detected.

The potential therapeutic benefit of MSCs can only be realized through their homing efficiency to the required site. The homing of MSCs was detected by PKH26 dye which used to label MSCs [25].

Our results showed strong red auto fluorescence after transplantation into rats, confirming that these cells were actually insinuating themselves into the liver tissue as detected by fluorescent microscope. These results were in agreement with [13], who labeled bone marrow MSCs with PKH26 dye and administrated it as red fluorescence of the MSCs.

In this study, MSCs administration showed significant improvement in liver functions in treated group compared to cirrhotic one. Also, decreasing the collagen accumulation and hydroxyproline content that were observed in cirrhotic rats. The histopathological examination of liver tissue confirmed this result and showed that MSCs have a significant antifibrotic effect as evidenced by the disappearance of septal collagen deposition and diffuse and homogeneous PAS staining for glycogen.

[26] suggested that the disappearance of collagen content in the cirrhotic rats treated with MSCs was apparently due to the lysis of fibrotic tissue which was accomplished by MMP2 activity. Metalloproteinase (MMPs) more particularly the MMP2 that promote the degradation of extra cellular matrix (ECM) in liver cirrhosis should have been secreted by MSC, which in the presence of hepatic growth factor (HGF) exhibited increased matrix metalloproteinases 2 (MMP2) activity, as observed by enhanced fibrolysis and/or prevention of collagen synthesis. This would have facilitated the assembling and orientation of stem cells in the hepatic nodules where they can differentiate into functional hepatocytes.

Bone marrow derived MSCs have the ability to repair damaged liver [25] however; extensive fibrosis, scar development and lack of survival may influence regeneration ability. Strategies targeting removal of activated HSCs have shown to reduce fibrosis and augment liver function [28]. A combined approach aimed at specific removal of activated HSCs would improve hepatic milieu allowing MSCs to survive, engraft and differentiate into hepatocytes [29].

The underlying mechanisms in the modulation of HSC activity by MSC were attributed to paracrine mediators, IL-10, TNF- α and HGF. Blockade of MSC-derived IL-10 and TNF- α abolished the inhibitory effects of MSC on HSC proliferation and collagen synthesis; MSC-derived HGF was responsible for the marked induction of HSC apoptosis as determined by antibody neutralization studies. IL-6 secretion from activated HSCs induced IL-10 secretion from MSC, suggesting a dynamic response of MSC to HSCs in the microenvironment. HSC apoptosis can also be triggered by MSC-secreted nerve growth factor (NGF) stimulation [30].

Several animal studies and clinical trials have demonstrated that MSCs have the potential to reverse the fibrotic process by inhibiting collagen deposition and transforming growth factor- β 1 production. The molecular mechanism underlying the antifibrotic properties of MSCs can mainly reside in the high expression levels of matrix metalloproteinase (MMPs), especially MMP-9, which may directly degrade the extracellular matrix and lead to hepatic stellate cell apoptosis [31].

[32] stated that BM-derived stem cells may be one of the important sources for hepatocyte repair. Possible explanations are that, MSCs can repair tissues by three mechanisms: (1) by differentiating into the phenotype of the damaged cells; (2) by secreting growth factors and cytokines that enhances repair of endogenous cells; and (3) by undergoing cell fusion [33].

Differentiation of MSCs into the phenotype of the damaged cells was confirmed by [34] who reported that adipose tissue derived MSC have the endoderm differentiation capacity including insulin-, somatostatin-, and glucagon- expressing cells as well as ALB- and AFP-expressing hepatocyte-like cells with the ability to synthesize urea and uptake LDL.

This was explained by [35] who indicated that when MSCs administrated, it underwent transdifferentiation into hepatic oval cells and then to hepatocyte-like cells. During this process,

inflammation was reduced, damaged hepatocytes were repaired, and fibrosis was resolved, resulting in an overall improvement in liver function with a definite increase in intracellular glycogen storage.

Also, the primary BM-derived stem cells can undergo a process of differentiation and the differentiated cells express various hepatocyte-specific markers, and have hepatocyte-specific bioactivities, including urea production, albumin secretion and glycogen storage [36].

In addition to the transdifferentiation ability, soluble factors produced by MSCs may play an important role in regeneration and protection from hepatocellular death. It has been demonstrated that MSC-CM (MSC conditioned medium) has direct anti-apoptotic and pro-mitotic effects on cultured hepatocytes. Furthermore, an infusion of MSC-CM inhibited death of hepatocytes enhanced the liver regeneration in vivo, and, ultimately, improved survival in rats after D-galactosamine-induced fulminant hepatic failure [37].

Moreover, angiogenic support provided by MSC can be considered one more supportive effect, since the re-establishment of blood supply is fundamental for recovery of damaged tissues [38]. In addition, BM-derived cells change their gene expression pattern to that of mature functional hepatocytes through fusion with damaged recipient liver cells.

CONCLUSION

The potential of MSC for transdifferentiation, paracrine functions and fusion with damage recipient liver cells suggested that MSC based cell therapy could be used successfully for the treatment of liver inflammation and cirrhosis.

ACKNOWLEDGEMENT

Authors are grateful to the National Research Center, Giza, Egypt for unlimited help and support to carry out this work.

REFERENCES

1. Raju SBG, Battu RG, Manju latha YB, Srinivas K. Antihepatotoxic activity of *Smilax china* roots on CCl₄ induced hepatic damage in rats. International Journal of Pharmacy and Pharmaceutical Sciences 2012; 4(1): 494-496.
2. Lee WM, Squires RH, Nyberg SL, Doo E, Hoofnagle JH. Acute liver failure: summary of a workshop. Hepatology 2008; 47:1401-1415.
3. Kim W R, Kremers W K. Benefits of "the benefit model" in liver trans-plantation. Hepatology 2008; 48:697-698.
4. Serralta A, Donato M T, Martinez A, et al. Influence of preservation solution on the isolation and culture of human hepatocytes from liver grafts. Cell Transplant 2005; 14:837-843.
5. Almeida G, Zanjani D E, Porada D C. Bone marrow stem cells and liver regeneration. Experimental Hematology 2010; 38: 574-580.
6. Patel NR, Parik B V, Jain KD, Baviskar TD. Adult stem cell: a new therapy to treat heart failure. International Journal of Pharmacy and Pharmaceutical 2012; 4(4): 52-58.
7. Vassilopoulos G, Wang P R, Russell D W. Transplanted bone marrow regenerates liver by cell fusion. Nature 2003; 422: 901-904.
8. McTaggart S J, Atkinson K. Mesenchymal stem cells: immunobiology and therapeutic potential in kidney disease. Nephrology 2007;12: 44-52.
9. Abdel Azia MT, Atta HM, Mahfouz S, Fouad HH, Roshdy NK, Ahmed HH, Rashed LA, Sabry D, Hassouna AA, Hasan NM. Therapeutic potential of bone marrow derived mesenchymal stem cells on experimental liver fibrosis. Clinical Biochemistry 2007; 40: 893-899.
10. Oe S., Fukunaka Y, Hirose T, Yamaoka Y, Tabata Y. A trial on regeneration therapy of rat liver cirrhosis by controlled release of hepatocyte growth factor. J of Controlled Release 2003 ; 88:193-200.
11. Alhadlaq A, Mao JJ. Mesenchymal stem cells: isolation and therapeutics. Stem Cells Dev 2004;13(4):436-48.

12. Bobis S, Jarocho D, Majka M. Mesenchymal stem cells: characteristics and clinical Applications. *Folia Histochemica Et Cytobiologica* 2006; 44(4): 215-230.
13. Munoz-Fernandez R, Blanco F J, Frecha C, Martin F, Kimatrai M, Abadia-Molina A C, Garcia-Pacheco J M, Olivares E. Follicular dendritic cells are related to bone marrow stromal cell progenitors and to myofibroblasts. *J Immunol G* 2006; 177: 280-289.
14. Wang G, Maher E, Brennan C, Chin L, Leo C, Kaur M, Zhu P, Rook M, Wolfe J L, Makrigrigors G M . DNA amplification method tolerant to sample degradation. *Genome Res* 2004 ; 14 (11): 2357-2366.
15. Marina M, Casiraghi F, Azzollini N, Cassis P, Imberti B, Cugini D, Cavinato RA, Todeschini M, Solini S, Sonzogni A, Perico, Remuzzi G, Noris M. Human bone marrow mesenchymal stem cells accelerate recovery of acute renal injury and prolong survival in mice. *Stem cells* 2008; 26:2075-2082.
16. Lee JK, Jin HK, Bae JS. Bone marrow derived mesenchymal stem cells reduce brain amyloid-beta deposition and accelerate the activation of microglia in an acutely induced Alzheimer's disease mouse model. *Neurosci Lett*. 2009; 450:136-141.
17. Reitman S, Frankel S. A colorimetric method for the determination of serum glutamic oxalacetic and glutamic pyruvic transaminases. *Amer J Clin path* 1957; 28-56.
18. Dumas BT, Watson WA, Biggs HG. Albumin standards and the measurement of serum albumin with bromocresol green. *Clin Chim Acta* 1971; 31:87-96.
19. Passing H, Balok WA. New biometrical procedure for testing the equality of measurements from two different analytical methods. *J clin biochem* 1993; 21:709-720.
20. Patiyal SN, katoch S S. Tissue Specific and Variable Collagen Proliferation in Swiss Albino Mice Treated with Clenbuterol. *Physiol Res* 2006; 55: 97-103.
21. Ala-Kokko L, Pihlajaniemi T, Myers JC, Kivirikko KI, Savolainen ER. Gene expression of type I,III and IV collagens in hepatic fibrosis induced by dimethylnitrosamine in the rat. *Biochem J* 1987; 15:244(1):75-9.
22. Drury AR, Wallington EA: Carleton's histological techniques 5th ed. University Press. London 1980; 140.
23. Hatakeyama Y, Onon T, Sato N, Sakuma H, Koyama Y, Inoue N, Takeenoshita S, Omata S. Usefulness of the tactile sensor for estimating the degree of liver fibrosis and the DNA synthesis activity of remnant liver cells after partial hepatectomy. *Fukushima J Med Sci* 2002; 48: 93-101.
24. Sanz N, Di'ez-Ferna'ndez C, Andre's, Mari'a Cascales D. Hepatotoxicity and aging: endogenous antioxidant systems in hepatocytes from 2-, 6-, 12-, 18- and 30-month-old rats following a necrogenic dose of thioacetamide. *Biochimica et Biophysica Acta* 2002; 1587:12- 20.
25. Li D, Xu S, Liu Y, Zhang S, Feng Y, Dai L. Cell-Based Therapy of Liver Cirrhosis. *Advances in Medicine and Biology* 2009; 7:1-32.
26. Ries C, Egea V, Karow M, Kolb H, Jochum M, Neth P. MMP-2, MTI-MMP. and TIMP-2 are essential for the invasive capacity of human mesenchymal stem cells: differential regulation by inflammatory cytokines. *Blood* 2007; 109:4055-4063.
27. Alison M., Islam S, Lim S. Stem cells in liver regeneration, fibrosis and cancer: the good, the bad and the ugly. *J Pathol* 2009; 217:282-298.
28. Moreno M, Gonzalo T, Kok RJ, Sancho-Bru P, Beuge MV, Swart J, Prakash J, Temming K, Fondevila C, Beljaars L, Lacombe M, Hoeven PVD, Arroyo V, Poelstra K, Brenner DA, Gines P, Bataller R. Reduction of advanced liver fibrosis by short-term targeted delivery of an angiotensin receptor blocker to hepatic stellate cells in rats. *Hepatology* 2010; 51:1-11.
29. Ali G, Mohsin S, Khan M, Nasi AG, Shams S, Khan NS, Riazuddin S. Nitric oxide augments mesenchymal stem cell ability to repair liver fibrosis. *Journal of Translational Medicine* 2012; 10:75.
30. Chen X, Li Y, Wang L, Katakowski M, Zhang L, Chen J, Xu Y, Gautam SC, ChoppM. Ischemic rat brain extracts induce human marrow stromal cell growth factor production. *Neuropathol* 2002; 22: 275-279.
31. Tsai P C, Fu T W, Chen Y M A et al. The therapeutic potential of human umbilical mesenchymal stem cells from Wharton's jelly in the treatment of rat liver fibrosis. *Liver Transplantation*(2009); 15 (5): 484-495.
32. Alison MR, Poulson R, Jeffery R, Dhillon AP, Quaglia A, Jacob J, Novelli M, Prentice G, Williamson J, Wright NA. Hepatocytes from non-hepatic adult stem cells. *Nature* 2000; 406:257-283.
33. Prockop DJ, Gregory CA, Spees JL. One strategy for cell and gene therapy: harnessing the power of adult stem cells to repair tissues. *Proc Natl Acad Sci* 2003; 100: 11917-11923.
34. Timper K, Seboek D, Eberhardt M, Linscheid P, Christ-Crain M, Keller U, et al. Human adipose tissue-derived mesenchymal stem cells differentiate into insulin, somatostatin, and glucagon expressing cells. *Biochem Biophys Res. Commun* 2006;341:1135-1140.
35. Hwang S, Hong HN, Kim HS, Park S R, Won YJ, Choi ST, Choi D, Lee SG Hepatogenic differentiation of mesenchymal stem cells in a rat model of thioacetamide induced liver cirrhosis. *Cell Biology International* 2012; 36(3):279-88.
36. Lee KD, Kuo T, Chung YF, Lin CT, Chou SH, Chen JR . In vitro hepatic differentiation of human mesenchymal stem cells. *Hepatology* 2004; 40: 1275-1284.
37. Van Poll D, Parekkadan B, Cho CH, Berthiaume F, Nahmias Y, Tilles AW, Yarmush ML. Mesenchymal stem cell-derived molecules directly modulate hepatocellular death and regeneration in vitro and *in vivo*. *Hepatology* 2008; 47: 1634-1643.
38. Sorrell JM, Baber MA, Caplan AI .Influence of adult mesenchymal stem cells on in vitro vascular formation. *Tissue Eng Part A* 2009; 15(7):1751-61.